Advances in Science and Technology
Research Journal

Advances in Science and Technology Research Journal 2022, 16(4), 201–210
https://doi.org/10.12913/22998624/152790
ISSN 2299–8624, License CC-BY 4.0

Received: 2022.07.01
Accepted: 2022.08.14
Published: 2022.09.01

Microstructure and Hardness of Cold Forged 42CrMo4 Steel Hollow Component with the Outer Flange

Mirosław Szala[1*], Grzegorz Winiarski[2], Tomasz Bulzak[2], Łukasz Wójcik[2]

[1] Department of Materials Engineering, Mechanical Engineering Faculty, Lublin University of Technology, Poland, Nadbystrzycka 36, 20-618, Lublin, Poland

[2] Department of Metal Forming Technologies, Mechanical Engineering Faculty, Lublin University of Technology, Nadbystrzycka 36, 20-618 Lublin, Poland

* Corresponding author's e-mail: m.szala@pollub.pl

ABSTRACT

For decades, steel has been a crucial structural material. Mainly low-alloy steel grade 42CrMo4 is utilized for manufacturing forgings. This paper investigates the microstructure and hardness development of the 42CrMo4 steel hollow component with an outer flange. The component has been formed via cold forging in combination with extrusion and upsetting technologies. Prior to forming, the workpiece was annealed to obtain hardness at the level of 181±9 HV0.3. The FEM analysis reveals the areas that undergo higher stress and strain. The flow lines macrostructure and microstructure of hollow parts were investigated using light optical microscopy (LOM) and scanning electron microscopy (SEM) equipped with EDS. Vickers hardness allows identifying the work hardening of the crucial element areas. The microstructure consists of ferrite matrix and semispherical carbides. Laboratory studies confirm appropriate flow lines arrangement, which corresponds well to those shown by FEM computer simulations. The highest hardness at the level of 293±7 HV0.3 was identified in the flange area, where the material shows a higher distribution of effective strain revealed by FEM. Cold metal forming results in work-hardening of the steel. The work hardening ranges up to 1.62 of the initial 42CrMo4 steel hardness. The metal forming process did not affect the microstructural uniformity of the flanged hollow part. The final outer flange component presents high quality and is free from plastic deformation nonuniformities.

Keywords: microstructure, hardness, strain hardening, steel, extrusion, metal forming, upsetting, FEM.

INTRODUCTION

For decades carbon and low alloy steels have been a crucial structural material due to their excellent combination of ductility and strength resulting from a heat treatment [1,2], specialized alloying additives [3,4] or specialized thermo-mechanical influencing on steel microstructure refinement [5,6]. One of the most popular steel utilized for forged components is low-alloy grade 42CrMo4 (AISI 4140). This steel can gain high mechanical properties [7,8], formality [9,10], or machinability [11,12] with the application of specific heat treatment [13,14]. Depending on the stage of element fabrication, 42CrMo4 steel can be softened, improving steel formality, or hardened to strengthen the final component's mechanical [15] or anti-wear properties [16]. However, the selection of appropriate treatment parameters is a complex process. Scientific literature reports the effects of plastic forming technology on the final steel part's microstructure, mechanical properties, and operational performance. It is known that steel formability is improved while reducing hardness. Therefore softening annealing treatment should be applied before cold forging [15]. Concerning time and costs, many different softening treatment programs have been implemented to optimize the annealing parameters of AISI 4140 steel [16,17]. It can be concluded that the selection of appropriate heat treatment is a multicriteria process taking into account, among others, the size of the component, initial steel structure, and aimed final mechanical properties. Moreover, Bounezour et al. [18] study the effect of work hardening on the mechanical properties of steel and aluminum alloy. It has been concluded that depending on the considered metals, when the piece has a defect variation: cavity, inclusion (precipitate), or zones of different hardness, it can create a stress concentration that generates a local hardening. This phenomenon is one of the leading causes of crack generation. Many papers characterize the stress-strain curves as essential to describe the plastic behavior of steel. Interesting results have been obtained by Li et al. [19], who proposed a formula that describes the full range strain hardening behavior of steels. Besides, microstructure analysis is crucial for the evaluation of the effects of initial heat treatment for plastic processes [20,21], the quality of plastic forming processes [22], or identifying the macro- and microstructure nonuniformities [23,24]. Therefore in the current paper, all mentioned features were considered while evaluating the quality of the fabricated hollow part.

The mechanical properties of the forged elements rely not only on the steel grade or heat treatment but are strongly affected by the parameters forging process itself. Inappropriate forging technology can result in nonuniform flow lines arrangement and microstructural discontinuities acting as internal notches. These could disturb the machining process or further deteriorate the components' operational performance, significantly limiting their mechanical performance likewise fatigue resistance [25,26]. It is known that cold forming processes modify the microstructure and strain hardened the deformed steel [27]. The high rate of strain hardening of the forging makes further stages of metal forming impossible and requires inter-forging annealing. This elongates the total forming time and consequently generates additional costs. Therefore, evaluating the microstructure and strain hardening of the forging part seems essential while introducing the plastic metal forming technology.

This work is another step to optimize the metal forming process of manufacturing hollow components with outer flange [28–31]. The innovative technology relies on cold forging in combination with extrusion and upsetting methods. The process was investigated via numerical simulations and positively verified experimentally on the model aluminum alloy [32]. The elaborated novel metal forming process is dedicated to manufacturing elements of 42CrMo4 steel. Therefore to assess the elaborated technology, it is necessary to investigate the quality of the 42CrMo4 steel hollow component. The study aims to investigate the quality of the final forging by evaluating the microstructure development and work hardening level in the forging part crucial areas. This is especially important for assessing the effectiveness of metal forming and heat treatment (annealing) operations, which contribute to elaborating the cost-effective technological process for manufacturing hollow components with outer flange.

MATERIAL AND METHODS

Forging of the hollow steel component with an outer flange

The object of the study was a hollow component with an outer flange made of 42CrMo4 (1.7225) steel (the equivalent of AISI 4140 grade). The main chemical composition of steel is given in Table 1. The final element is shown in Figure 1. Figure 2 shows the main steps of the component forming. The forming process is a combination of extrusion and upsetting. More details regarding the evolution of the idea of elaborated metal forming technology are presented in previous papers [30,32–34]. The current study physically modeled the metal forming process in laboratory conditions using a 1:2.5 scale of die tools. The further goal of the project is to obtain the aimed hollow part dimensions given in Figure 1.

The softening annealing preceded the metal forming of 42CrMo4 billet. The heat treatment procedure was investigated in a previous

Table 1. Chemical composition (cast analysis) of 42CrMo4 steel according to the EN 10083–3: Steels for quenching and tempering. Part 3: Technical delivery conditions for alloy steels

Chemical composition % by mass						
C	Mn	Si	Cr	Mo	S	P
0.38–0.45	0.6–0.9	<0.4	0.9–1.2	0.15–0.3	< 0.035	< 0.025

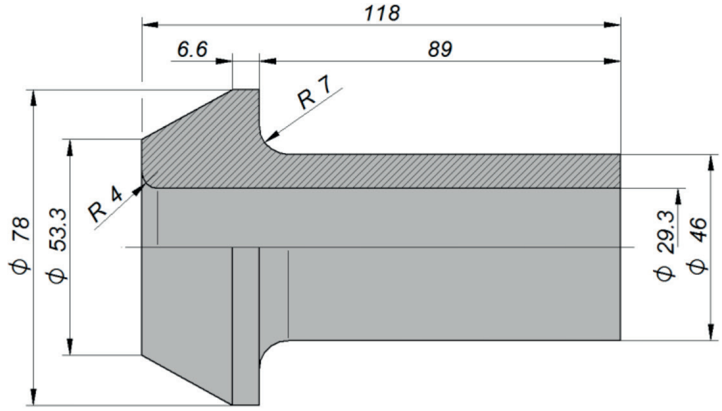

Fig. 1. Dimensions of the 42CrMo4 steel hollow component with the outer flange [35]

paper [10], and accordingly, scheme no. 1 was selected, see Fig. 3. This treatment enables the reduction of as-received 42CrMo4 steel hardness from 355 HV0.3 to 165 HV0.3 which effectively increases the steel deformability.

FEM analysis of a component at different stages of forming

FEM method was employed to select the specific hollow component areas for microstructure and hardness investigations. First, numerical calculations were performed using Deform 2D/3D according to the procedure shown in [36]. Then, the distribution of strain, stress, and flow lines arrangement were computationally analyzed at different stages of forming utilizing the FEM simulation results of components similar to those proposed in the current study. Finally, the highest strained and deformed structures were identified as crucial areas for microstructure and hardness analysis.

Microstructural and hardness methodology

The macrostructure and microstructure were comparatively analyzed at different stages of forming, using a standard metallographic methodology. Jacewicz's reagent (12 ml sulphuric acid, 38 ml hydrochloric acid, and 50 ml distilled water) was used to reveal the flow lines arrangement at different stages of forming (macroetching) and Nital (95–99 ml ethanol and 1–5 ml nitric acid) was used to show the steel microstructure. The areas of interest for the microstructure and hardness investigations were chosen via analysis of FEM flow lines, stresses, and strain distributions. Therefore, three specific locations were selected: the flange top, flange center, and sleeve areas of the hollow component with an outer flange. Metallographic specimens were observed using LOM (light optical microscopy) and SEM-EDS methods. Vickers hardness (HV0.3) was measured according to the ISO 6507 standard, using 10 seconds of dwelling time. Seven indentations

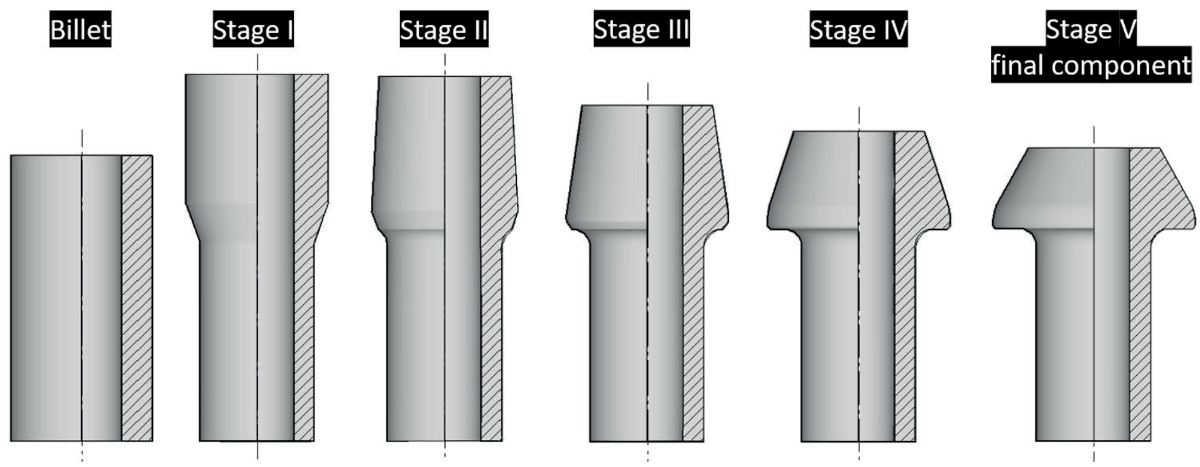

Fig. 2. Idea of the five stages forming process: I stage – extrusion, II-V stages – flange upsetting

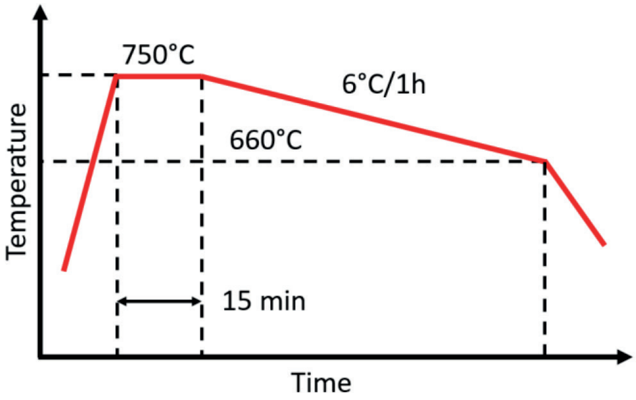

Fig. 3. Annealing process parameters utilized for 42CrMo4 sleeve batch

were made in each investigated area to obtain statistical accuracy. Generally, when a metal or alloy is being worked below the recrystallization temperature, the material becomes strengthened and hardened but decreases in ductility. Such a process is called work/strain hardening. Hardness tests reveal the strain hardening (estimated as the relation of the strained component hardness to the initial annealed hardness). The level of strain hardening is essential for further manufacturing and performance of the component. Therefore, the flow lines, non-uniformities, chemical composition, microstructure and grain arrangement, and hardness were investigated experimentally to identify the final component's quality.

RESULTS AND DISCUSSION

FEM results of strain (Fig. 4), stress and the flow lines analysis with the revealed flow lines at different stages of cold-forming. While the component fabricated in laboratory conditions at different stages of metal deformation are shown in Figure 5. In Figure 7, the results of the macroscopic metallography are shown. The areas of the highest stress and strain localized by FEM (i.e., flange center) correlate with the flow lines arrangement. Therefore, it seems that these areas should show the highest level of strain hardening (discussed further). Therefore, the hollow component's flange top, center, and sleeve were chosen for hardness analysis. Moreover, a comparison of the simulated and revealed by the metallography investigations (Fig. 7) indicate a similar flow lines arrangement. The detailed microscopic investigation confirmed the high quality of the forging part. The flow lines show appropriate morphology and arrangement. Elements are free from plastic deformation nonuniformities. Therefore, the satisfactory macrostructure of the forged components has been obtained.

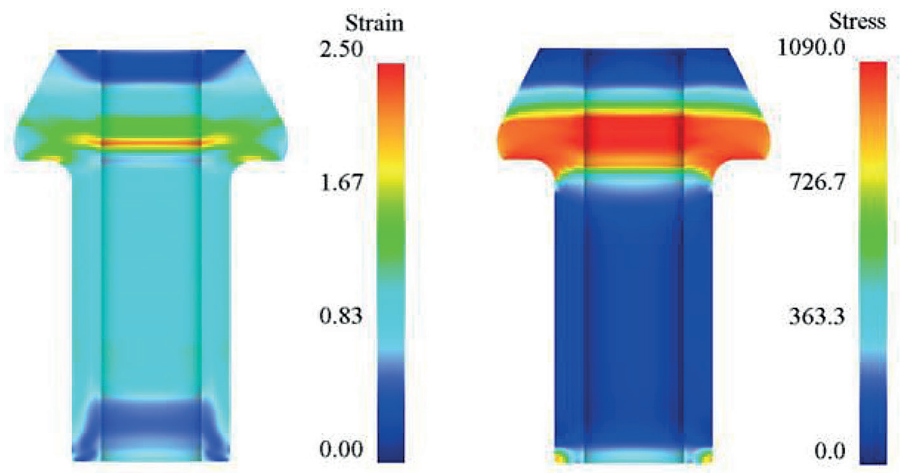

Fig. 4. The forging's highest strain and stress areas at the final stage of cold-forming, following the results of comparable forming technology [36], FEM

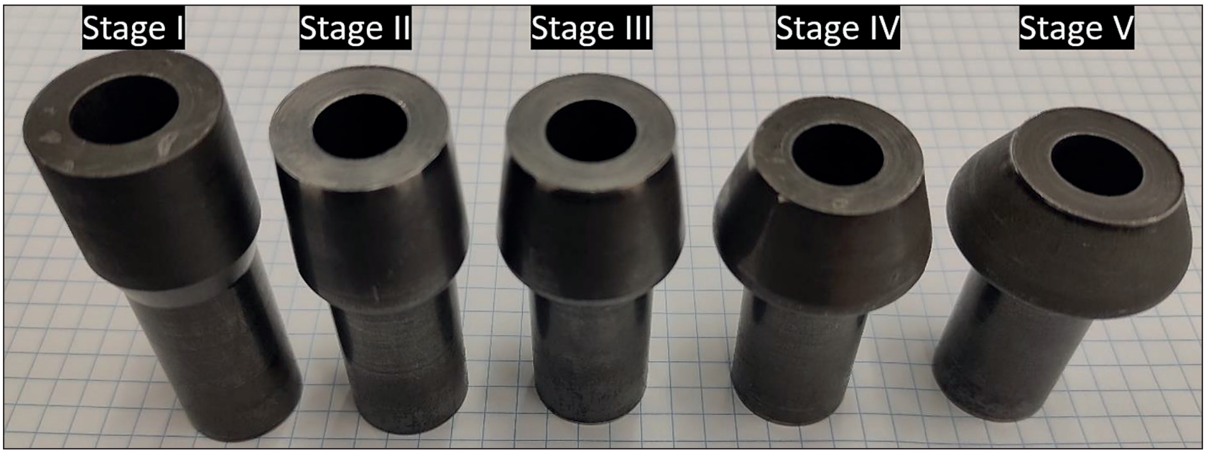

Fig. 5. Fabricated forgings at five stages of forming

The as-received microstructure of 42CrMo4 steel consisted of ferrite and perlite (lamellar structure composed of alternating layers of cementite and ferrite, Fig. 8a). The utilized annealing treatment program resulted in the formation of a ferrite matrix with fine semispherical carbides, see Fig. 8b. Obtained microstructure facilitates cold metal forming processes. Besides, the development of the structure due to annealing agrees with those discussed in the author's previous research [10]. The microstructure of the final component has been observed in the areas shown in Fig. 9 and Fig. 10. LOM and SEM analysis indicate differences in grain flow between specific areas of the component. The presence of the coarse carbides is typical for high alloy tool steels [37,38], while in the case of low alloy steel, the Mn, Cr, and Mo would partition to cementite [39]. Similarly, the increased content of Mo, Mn, and Cr was identified in carbides, Fig. 9c. Furthermore, SEM-EDS analysis (Fig. 9) confirms the presence of nonmetallic inclusions, i.e., manganese sulfide type (MnS) typical for structural steels [40]. This type of inclusion could deteriorate the forging properties' uniformity, significantly lowering the fracture and fatigue resistance [26]. However, presented investigations indicate that applied deformation (due to cold forming) does not affect structure uniformity negatively. Neither voids nor cracking of metallic matrix was observed. Analysis of flow lines indicated differences in arrangement relating to the specific area of the hollow part (Fig. 10). In the sleeve area, ferrite grains are elongated parallel to the central axis of the rotary part. The extrusion process is responsible for sleeve microstructure Fig. 10. Contrary to that, the center of the flange was fabricated by upsetting; therefore, ferrite grains are compressed. FEM analysis indicates the highest strain and stress in the center of the flange than in the flange top, see Fig. 4. Metallographic study confirms that ferrite grains are less deformed on the flange top than in the center of the flange (Fig. 10). Besides, the microstructural homogeneity in the sleeve area reflected a homogeneous distribution of strain, visualized by FEM.

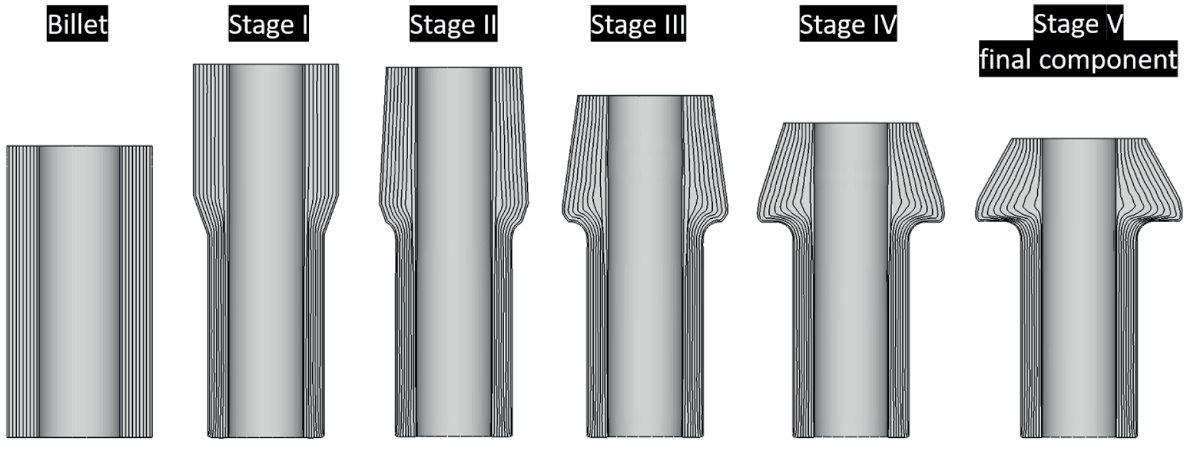

Fig. 6. Simulation of flow lines arrangement at different stages of forming, FEM

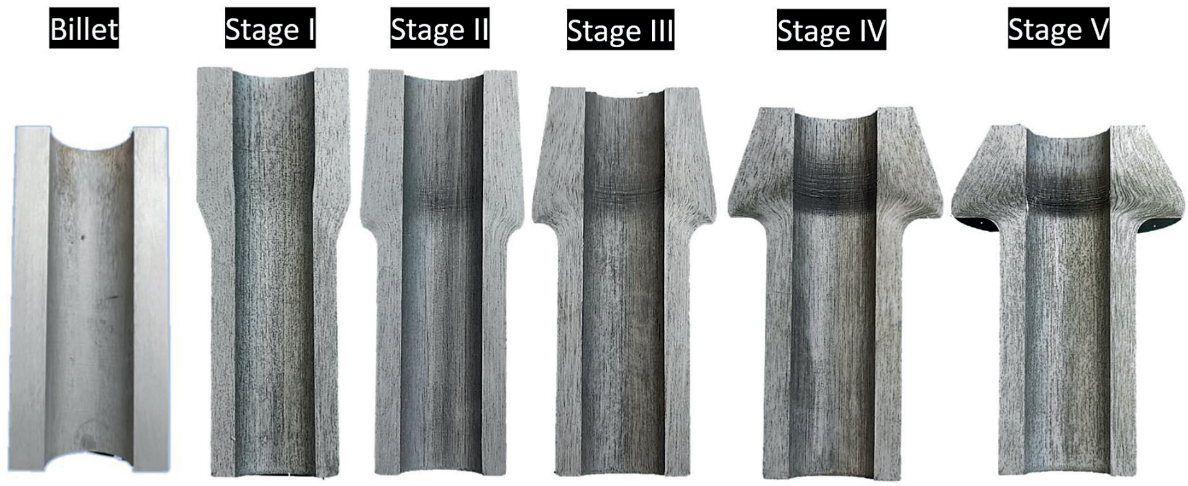

Fig. 7. Macrostructure of a hollow flanged component at different stages of forming, macroetching

The rate of plastic deformations indicates steel work hardening and hardness fluctuations. The Vickers hardness was measured before and after metal forming. Thus, applied heat treatment reduces the hardness of the billet to 181±9 HV0.3 (Fig. 11), which slightly exceeds the minimal hardness obtained for model cylinders investigated in the preliminary study [10]. Moreover, literature [16] reports that different hardness can be obtained after spheroidization annealing of AISI4140 steel and final hardness strongly relates to initial heat treatment and microstructure [41]. Exemplary, E. Karadeniz [16] find out that initially hardening and subcritical spheroidization method application give greater forgeability values in a short time, so it is preferable in cold forging production from AISI 4140 steel for time and cost [16]. However, it was also concluded that the drop in the spheroidised steel hardness rate between the initially normalized and hardened process is much less [16]. Cold forming resulted in strain hardening of the flange center to 293 HV0.3 (Fig. 10), corresponding to a strain hardening level of 1.62. The hardness of the sleeve area formed at the first stage of the process (extrusion) gained approx.. 40 HV lower values than the maximal hardness recorded for the flange center. The flange was formed via upsetting. This level of strain hardening does not exceed the maximal value reported for the upsetting of 42CrMo4 cylinder specimens [10]. It confirms that the elaborated metal forming technique gives hardening at an acceptable level. The central flange area shows the highest strain hardening resulting from severe structure deformation. In contrast, the top flange area was less hardened (Fig. 11). This well correlates with flow lines arrangement (Fig. 7) and microstructure development (Fig. 10). Summing up, both metallographic and hardness investigations confirm that the elaborated metal forming

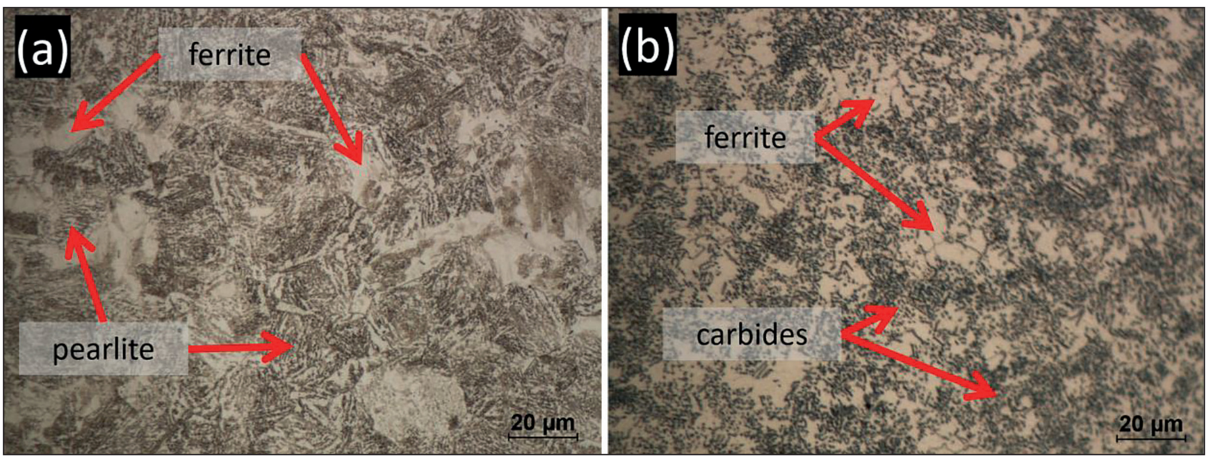

Fig. 8. Effect of annealing on the microstructure of the 42CrMo4 steel. As-received (a) and (b) annealed steel, LOM

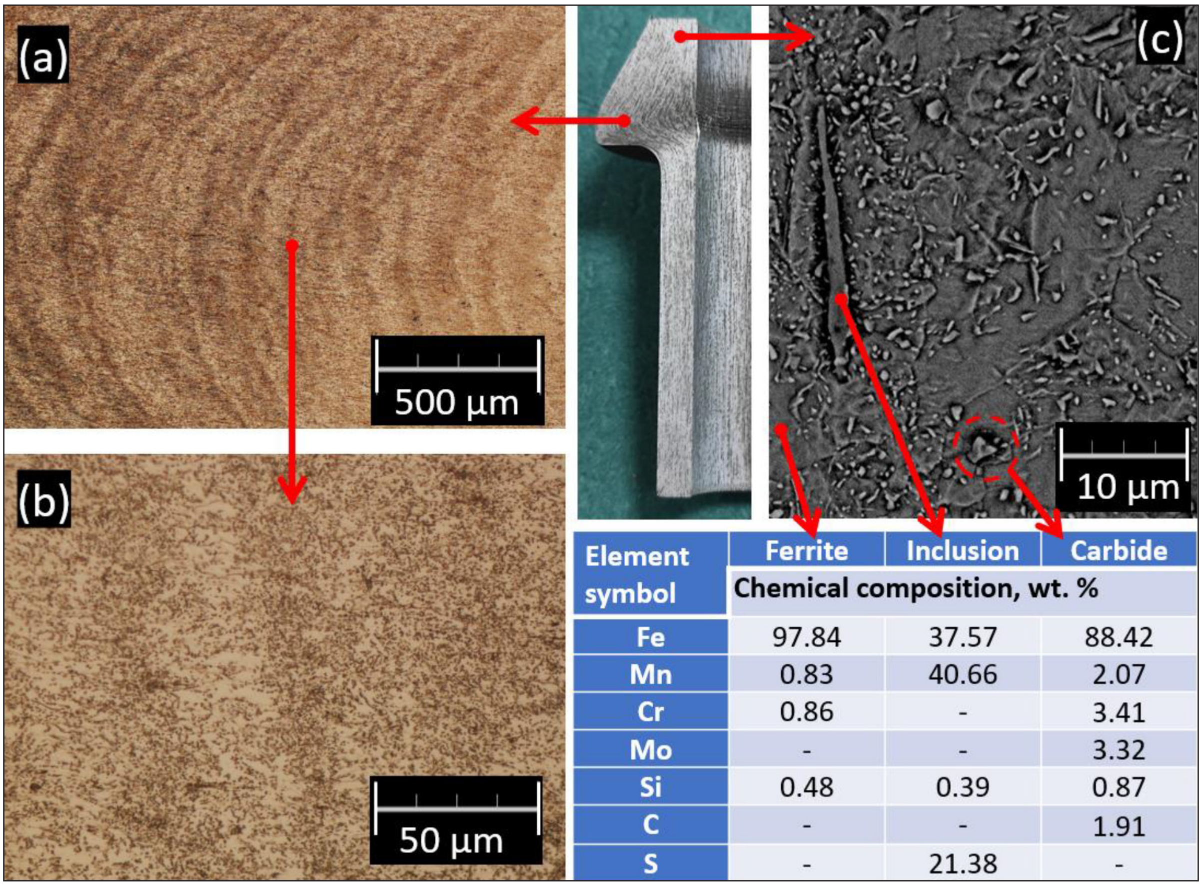

Element symbol	Ferrite	Inclusion	Carbide
	Chemical composition, wt. %		
Fe	97.84	37.57	88.42
Mn	0.83	40.66	2.07
Cr	0.86	-	3.41
Mo	-	-	3.32
Si	0.48	0.39	0.87
C	-	-	1.91
S	-	21.38	-

Fig. 9. Macro- and microstructure in different areas of plastic deformation (a, b) LOM; (c) microstructure and results of spot chemical analysis, SEM-EDS

technique allows obtaining high quality of the flanged hollow parts made of 42CrMo4 steel. Therefore, the elaborated metal forming technique can be implemented for producing flanged hollow parts for the mining industry.

CONCLUSIONS

In the current work, the results of the investigation on the quality of forging parts made of steel 42CrMo4 were studied. Analysis reveals the microstructure and hardness development of the forged component at different stages of forging, which allows assessment of the proposed technology of the cold forging process in combination with extrusion and upsetting. As a result, the following findings are drawn:

- Applied annealing reduces the hardness of the billet to the level of 181±9 HV0.3 and modifies the initial pearlite-ferrite microstructure to the microstructure consisting of a ferrite matrix and semispherical carbides.
- Laboratory metallographic studies confirm appropriate flow lines arrangement, which arrangement well corresponds to those shown by FEM computer simulations
- The cold metal forming process results in different strain hardening levels noted in specific areas of the component. The highest hardness at 293±7 HV0.3 was identified in the flange area, where the material shows the higher distribution of effective strain revealed by FEM. The maximal strain hardening reached up to 1.62, and it did not negatively affect the microstructural uniformity of the flanged hollow part.
- The final component presents high quality and is free from plastic deformation nonuniformities.

Acknowledgements

The research was financed in the framework of the project: New metal forming technique for producing flanged hollow parts for the mining industry, No. LIDER/1/0003/L-9/17/NCBR/2018. Total cost of the Project: 1197000 PLN. The project is financed by the National Centre for Research and Development under the 9th edition of the LIDER Programme.

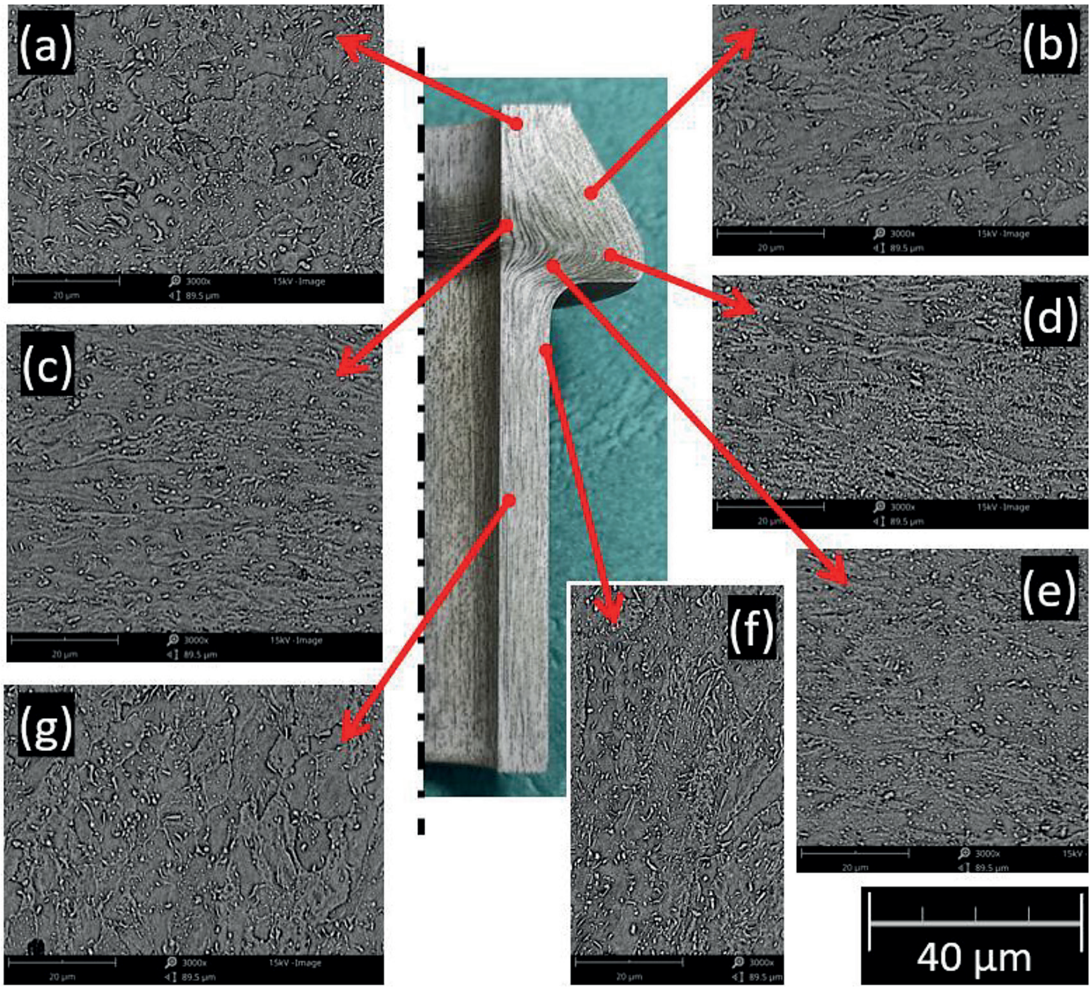

Fig. 10. Microstructure and grain arrangement in different locations of final component cross-section: flange top (a, b); flange center (c-e); sleeve (g, h), SEM

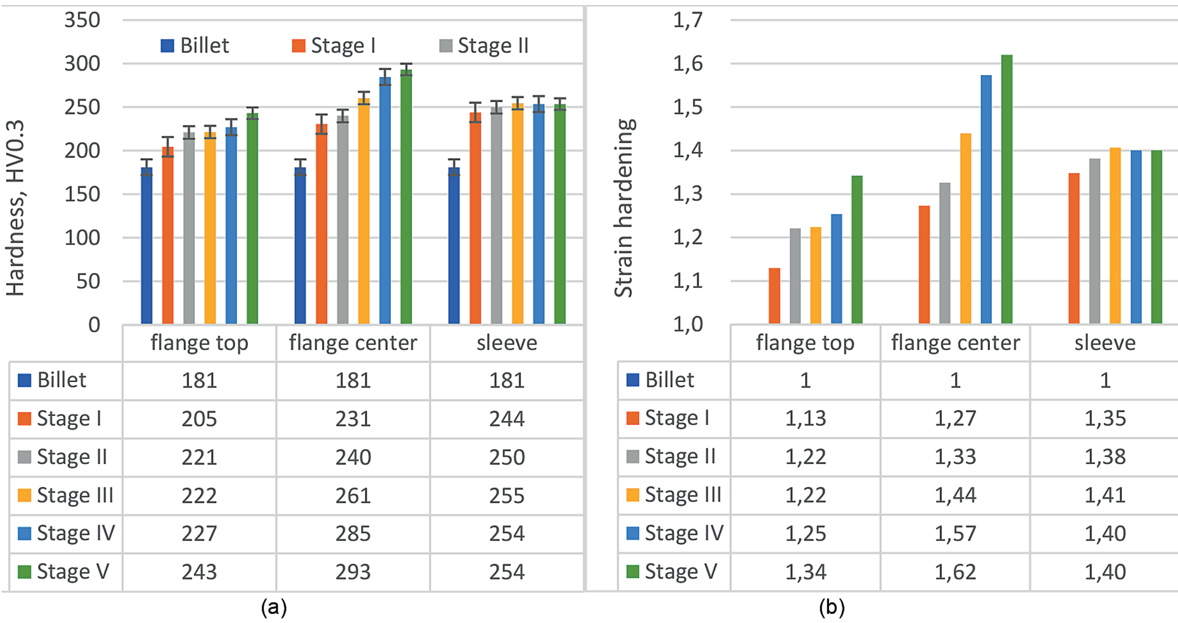

	flange top	flange center	sleeve
Billet	181	181	181
Stage I	205	231	244
Stage II	221	240	250
Stage III	222	261	255
Stage IV	227	285	254
Stage V	243	293	254

	flange top	flange center	sleeve
Billet	1	1	1
Stage I	1,13	1,27	1,35
Stage II	1,22	1,33	1,38
Stage III	1,22	1,44	1,41
Stage IV	1,25	1,57	1,40
Stage V	1,34	1,62	1,40

Fig. 11. Hardness results of specific areas of cold-formed hollow parts: (a) Vickers hardness; (b) strain hardening at different stages of metal forming

REFERENCES

1. E. Gadalińska, A. Baczmański, C. Braham, G. Gonzalez, H. Sidhom, S. Wroński, T. Buslaps, K. Wierzbanowski, Stress localisation in lamellar cementite and ferrite during elastoplastic deformation of pearlitic steel studied using diffraction and modelling, International Journal of Plasticity. 127 (2020) 102651. https://doi.org/10.1016/j.ijplas.2019.102651.
2. M. Duda, D. Rozumek, G. Lesiuk, M. Smolnicki, B. Babiarczuk, J. Warycha, Fatigue crack growth under mixed-mode I+II and I+III in heat treated 42CrMo4 steel, Int J Fract. 234 (2022) 235–248. https://doi.org/10.1007/s10704–021–00585–0.
3. B. Białobrzeska, Effect of Alloying Additives and Microadditives on Hardenability Increase Caused by Action of Boron, Metals. 11 (2021) 589. https://doi.org/10.3390/met11040589.
4. Ł. Konat, R. Jasiński, B. Białobrzeska, Ł. Szczepański, Analysis of the static and dynamic properties of wear-resistant Hardox 600 steel in the context of its application in working elements, Materials Science-Poland. 39 (2021) 86–102. https://doi.org/10.2478/msp-2021–0007.
5. W. Macek, Fracture Areas Quantitative Investigating of Bending-Torsion Fatigued Low-Alloy High-Strength Steel, Metals. 11 (2021) 1620. https://doi.org/10.3390/met11101620.
6. J. Tomków, A. Czupryński, D. Fydrych, The Abrasive Wear Resistance of Coatings Manufactured on High-Strength Low-Alloy (HSLA) Offshore Steel in Wet Welding Conditions, Coatings. 10 (2020) 219. https://doi.org/10.3390/coatings10030219.
7. C. Sun, P.-X. Fu, H.-W. Liu, H.-H. Liu, N.-Y. Du, Effect of Tempering Temperature on the Low Temperature Impact Toughness of 42CrMo4-V Steel, Metals. 8 (2018) 232. https://doi.org/10.3390/met8040232.
8. V. Malau, W.I. Fauzi, Effects of Heat Treatments on Mechanical Properties, Specific Wear and Corrosion Rate of HQ 809 Steel for Machinery Components Application, in: 2018 4th International Conference on Science and Technology (ICST), 2018: pp. 1–6. https://doi.org/10.1109/ICSTC.2018.8528600.
9. J.S. Kimm, J.A. Bergmann, F. Wöste, F. Pöhl, P. Wiederkehr, W. Theisen, Deformation behavior of 42CrMo4 over a wide range of temperatures and strain rates in Split-Hopkinson pressure bar tests, Materials Science and Engineering: A. 826 (2021) 141953. https://doi.org/10.1016/j.msea.2021.141953.
10. M. Szala, G. Winiarski, Ł. Wójcik, T. Bulzak, Effect of Annealing Time and Temperature Parameters on the Microstructure, Hardness, and Strain-Hardening Coefficients of 42CrMo4 Steel, Materials. 13 (2020) 2022. https://doi.org/10.3390/ma13092022.
11. N. Troß, J. Brimmers, T. Bergs, Tool wear in dry gear hobbing of 20MnCr5 case-hardening steel, 42CrMo4 tempered steel and EN-GJS-700–2 cast iron, Wear. 476 (2021) 203737. https://doi.org/10.1016/j.wear.2021.203737.
12. P.B. Zaman, M.N. Sultana, N.R. Dhar, Multivariant hybrid techniques coupled with Taguchi in multi-response parameter optimisation for better machinability of turning alloy steel, Advances in Materials and Processing Technologies. 0 (2021) 1–21. https://doi.org/10.1080/2374068X.2021.1945302.
13. ASM Handbook: Vol. 4: Heat Treating, 10 Edition, ASM International, Materials Park, Ohio, 1991.
14. M.M. Blaoui, M. Zemri, A. Brahami, Effect of heat treatment parameters on mechanical properties of medium carbon steel, Mechanics and Mechanical Engineering. Vol. 22 (2018). http://yadda.icm.edu.pl/yadda/element/bwmeta1.element.baztech-087c26c2–2c73–4e7a-b73d-ecd871983f8b (accessed July 26, 2022).
15. W. Woźniak, M. Sąsiadek, T. Jachowicz, M. Edl, P. Zając, Studies on the Mechanical Properties of C45 Steel with Martensitic Structure after a High Tempering Process, Adv. Sci. Technol. Res. J. 16 (2022) 306–315. https://doi.org/10.12913/22998624/150564.
16. E. Karadeniz, Influence of different initial microstructure on the process of spheroidization in cold forging, Materials & Design. 29 (2008) 251–256. https://doi.org/10.1016/j.matdes.2006.11.015.
17. E. Hao, Y. An, X. Liu, Y. Wang, H. Zhou, F. Yan, Effect of annealing treatment on microstructures, mechanical properties and cavitation erosion performance of high velocity oxy-fuel sprayed NiCoCrAlYTa coating, Journal of Materials Science & Technology. 53 (2020) 19–31. https://doi.org/10.1016/j.jmst.2020.03.030.
18. H. Bounezour, L. Laouar, M. Bourbia, B. Ouzine, Effects of work hardening on mechanical metal properties–experimental analysis and simulation by experiments, Int J Adv Manuf Technol. 101 (2019) 2475–2485. https://doi.org/10.1007/s00170–018–3071-x.
19. T. Li, J. Zheng, Z. Chen, Description of full-range strain hardening behavior of steels, Springerplus. 5 (2016). https://doi.org/10.1186/s40064–016–2998–3.
20. P. Yadav, K.K. Saxena, Effect of heat-treatment on microstructure and mechanical properties of Ti alloys: An overview, Materials Today: Proceedings. 26 (2020) 2546–2557. https://doi.org/10.1016/j.matpr.2020.02.541.

21. M. Kang, M. Park, B. Kim, H.C. Kim, J.B. Jeon, H. Kim, C.Y. Choi, H.S. Park, S.-H. Kwon, B.J. Kim, Effect of Heat Treatment on Microstructure and Mechanical Properties of High-Strength Steel for in Hot Forging Products, Metals. 11 (2021) 768. https://doi.org/10.3390/met11050768.
22. P. Widomski, M. Zwierzchowski, A. Barełkowski, M. Tympalski, Case study of the effect of precoating on the decarburization of the surface layer of forged parts during the hot die forging process, Materials. 14 (2021) 422. https://doi.org/10.3390/ma14020422.
23. T. Bulzak, K. Majerski, J. Tomczak, Z. Pater, Ł. Wójcik, Warm skew rolling of bearing steel balls using multiple impression tools, CIRP Journal of Manufacturing Science and Technology. 38 (2022) 288–298. https://doi.org/10.1016/j.cirpj.2022.05.007.
24. Z. Gronostajski, M. Hawryluk, P. Jabłoński, M. Zwierzchowski, A. Barelkowski, P. Widomski, The Effect of Heat Treatment of Forgings Directly from the Forging Temperature on their Properties, Archives of Metallurgy and Materials. 65 (2020) 685–696. https://doi.org/10.24425/amm.2020.132807.
25. W. Macek, R.F. Martins, R. Branco, Z. Marciniak, M. Szala, S. Wroński, Fatigue fracture morphology of AISI H13 steel obtained by additive manufacturing, Int J Fract. (2022). https://doi.org/10.1007/s10704–022–00615–5.
26. M. Kowal, M. Szala, Diagnosis of the microstructural and mechanical properties of over century-old steel railway bridge components, Engineering Failure Analysis. 110 (2020) 104447. https://doi.org/10.1016/j.engfailanal.2020.104447.
27. S. Hashmi, Comprehensive Materials Finishing, Elsevier, Kidlington, Oxford, United Kingdom, 2017.
28. G. Winiarski, T.A. Bulzak, Ł. Wójcik, M. Szala, Effect of Tool Kinematics on Tube Flanging by Extrusion with a Moving Sleeve, Adv. Sci. Technol. Res. J. 13 (2019) 210–216. https://doi.org/10.12913/22998624/110741.
29. Ł. Wójcik, T. Bulzak, G. Winiarski, M. Szala, Numerical analysis of three-stage the forming process hollow forgings with an outer flange, Scientific Journals of the Maritime University of Szczecin. 134 (2020) 142–147. https://doi.org/10.17402/429.
30. T. Bulzak, G. Winiarski, Ł. Wójcik, M. Szala, Application of Numerical Simulation and Physical Modeling for Verifying a Cold Forging Process for Rotary Sleeves, J. of Materi Eng and Perform. (2021). https://doi.org/10.1007/s11665–021–06314-x.
31. A. Gontarz, G. Winiarski, Numerical and Experimental Study of Producing Two-Step Flanges by Extrusion with a Movable Sleeve, Archives of Metallurgy and Materials. 62 (2017). http://journals.pan.pl/dlibra/docmetadata?id=105047 DOI – 10.1515/amm-2017–0071.
32. G. Winiarski, Theoretical and experimental study on the effect of selected parameters in a new method of extrusion with a movable sleeve. Materials. 15 (2022) 4585. https://doi.org/10.3390/ma15134585.
33. G. Winiarski, T.A. Bulzak, Ł. Wójcik, M. Szala, A New Method of Flanges Extrusion in Hollow Products – Analysis of the Limiting Phenomena, Adv. Sci. Technol. Res. J. 14 (2020) 78–85. https://doi.org/10.12913/22998624/125508.
34. G. Winiarski, T. Bulzak, M. Szala, Numerical analysis of a two-stage forming process for a hollow part with external flange, J. Phys.: Conf. Ser. 1736 (2021) 012005. https://doi.org/10.1088/1742–6596/1736/1/012005.
35. G. Winiarski, T. Bulzak, L. Wójcik, M. Szala, Cold forging of a hollow flanged part by an unconventional extrusion method, J. Phys.: Conf. Ser. 2130 (2021) 012019. https://doi.org/10.1088/1742–6596/2130/1/012019.
36. G. Winiarski, T.A. Bulzak, Ł. Wójcik, M. Szala, Numerical Analysis of a Six Stage Forging Process for Producing Hollow Flanged Parts from Tubular Blanks, Adv. Sci. Technol. Res. J. 14 (2020) 201–208. https://doi.org/10.12913/22998624/116748.
37. K. Drozd, M. Walczak, M. Szala, K. Gancarczyk, Tribological Behavior of AlCrSiN-Coated Tool Steel K340 Versus Popular Tool Steel Grades, Materials. 13 (2020) 4895. https://doi.org/10.3390/ma13214895.
38. M. Kaszuba, P. Widomski, P. Białucki, A. Lange, B. Boryczko, M. Walczak, Properties of new-generation hybrid layers combining hardfacing and nitriding dedicated to improvement in forging tools' durability, Archiv.Civ.Mech.Eng. 20 (2020) 78. https://doi.org/10.1007/s43452–020–00080–8.
39. Y.X. Wu, W.W. Sun, X. Gao, M.J. Styles, A. Arlazarov, C.R. Hutchinson, The effect of alloying elements on cementite coarsening during martensite tempering, Acta Materialia. 183 (2020) 418–437. https://doi.org/10.1016/j.actamat.2019.11.040.
40. Y. Tanaka, F. Pahlevani, S.-C. Moon, R. Dippenaar, V. Sahajwalla, In situ characterisation of MnS precipitation in high carbon steel, Sci Rep. 9 (2019) 10096. https://doi.org/10.1038/s41598–019–46450-y.
41. B. L. Ferguson, Z. Li, A. M. Freborg, Modeling heat treatment of steel parts, Computational Materials Science. 34 (2005) 274–281. https://doi.org/10.1016/j.commatsci.2005.02.005.